DOI: 10.61782/fa.2023.1071

CORRELATION OF TYRE/ROAD NOISE MEASUREMENTS VIA MACHINE LEARNING ALGORITHMS

Bernhard Baumgartner[1*] **Andreas Fuchs**[1] **Manfred Haider**[1]
[1] Austrian Institute of Technology, 1210 Vienna, Austria

ABSTRACT

Tyre/road interaction is the main cause for noise emission when considering road vehicles travelling faster than approx. $60\,\mathrm{km/h}$. A multitude of aspects play a major role regarding the overall observed sound pressure level (SPL), i.e. speed, vehicle type, driving style and pavement type/condition. The latter, however, facilitates the possibility of independent tuning of acoustic properties, e.g. via diamond grinding of concrete pavements or open-graded asphalts. Investigations regarding possible emission reductions are often performed using trailers, wherein installed microphones record the rolling noise close to the tyre/road contact. Another option is the analysis of isolated, statistical pass-bys of cars and trucks. This paper investigates the relationships between different trailer-based measurement techniques according to RVS 11.06.64 (RVS-method) and to ISO 11819-2 (CPX-method), as well as between the CPX-method and the Pass-by-measurements following ISO 11819-2 (SPB-method) [1–3]. Comparisons and correlations of pavement dependent overall SPL and analyses of respective third-octave bands will be presented. This includes the use of unsupervised machine learning algorithms allowing the determination of relevant frequency bands of either method.

Keywords: *tyre/road noise, CPX RVS measurement, Pass-by measurement, machine learning*

****Corresponding author***: *bernhard.baumgartner@ait.ac.at.*

1. INTRODUCTION

Regarding the approval of low-noise pavements within the Austrian road network measurements according to the RVS-method are mandatory. This trailer-based technique utilizes a single PIARC-tyre with linear grooves (thus strongly deviating from conventional tyres), lacks of corrections targeting the tyre rubber hardness and dates back to 1997. Moreover, the more elaborate CPX-Method is applied internationally and incorporates a realistic P1 test tyre as well as several corrections regarding the recorded sound pressure level [4].
Both methods are feasible options for monitoring acoustic properties of large road sections, however, they provide limited information on road vehicles other than passenger cars. This quantification may be done according to the stationary measurement method ISO 11819-1, which describes the analysis of statistical pass-by events (SPB). An interior image of the RVS- and CPX-trailer as well as an exemplary setup of SPB measurements are given in figure 1. Main differences between both trailer-based rolling noise measurement techniques are listed in table 1.

Figure 1: Trailer-based rolling noise measurements according to RVS 11.06.64 (left) and ISO 11819-2 (center) and single pass-by measurement setup following ISO 11819-1 (right). The orange circles in the left image indicate the microphone positions according to the RVS-method.

Table 1: Overview of major normative differences between described trailer-based rolling noise measurements according.

		RVS	CPX
Tyres	Types	PIARC Maloya	P1 ASTM SRTT-tyres
	Dimensions	165 R15	P225/60R16:2014
	Number	single	set of two
	Load	4000 N	3200 N per tyre
	Pressure	230 kPa	200 kPa
Correc-tions	ShoreA	no	yes
	Temperature	road temperature	air temperature
	Trailer chassis	no	yes
	Speed	yes	yes
	Road Type	yes	yes
Micro-phones	Number	2	4 (two on each side)
	Positions	beside (90°) and behind (0°) the tyre	in front of (45°) and behind (-45°) the tyre
	final SPLs	SPL of rear microphone if higher otherwise energy-based avg. levels of microphone pair	energy-based avg. levels of microphone pairs
Limi tations	Temperature	air temperature between 10 C and 40 C	road temperature between 5 C and 30 C
	Minimum Length	500 m	20 m

To allow for statistical correlations of RVS∼CPX (whereing RVS and CPX levels are treated as independent and dependent variables, respectively) a rolling noise dataset of $1860.9\,\mathrm{km}$ was recorded for both trailers. Furthermore, 36 SPB-measurements were performed on 30 different spots in the Austrian road network, thus providing sufficient data for quantifying a CPX∼SPB relationship. The majority of corresponding CPX-measurements were conducted within a few weeks before/after the SPB-method, respectively.
The following part describes the dataset and analysis steps regarding the above measurements. Section 3 provides a detailed overview of both analyzed correlations in terms of overall and third-octave-band SPLs. Regarding possible frequency-dependent interrelations a principal component analysis (PCA), i.e. an unsupervised machine learning method, is presented.

2. MEASUREMENT DATASET

An overview of the considered highways via blue and green lines is given in figure 2. Depicted lines correspond to trailer-based analyses, red points show the position of SPB-measurements. The collected data proves to cover an extensive part of Austrian network of major roads.

2.1 Trailer Based Measurements

More than 95% of the trailer based measurements were performed simultaneously by driving in a convoy in order to minimize the effect of varying ambient conditions.

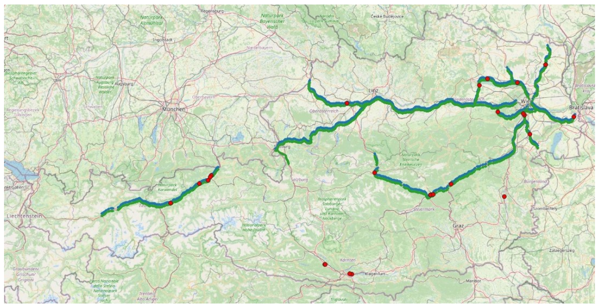

Figure 2: Highways analyzed via the RVS-method (blue) and CPX-method (green) as well as locations where SPB-data (red) is given.

Rolling noise, GPS-coordinates, speeds and temperatures of air, road and tyre were continuously recorded on a total of $1860.9\,\mathrm{km}$, see table 2. The single wheel of the RVS-trailer was kept within the right track of the first lane while the CPX-trailer covered both tracks of the first lane.

Table 2: Overview of the different road surfaces where trailer-based rolling noise measurements were performed according to RVS- and CPX-method with a measurement speed of $80\,\mathrm{km/h}$.

Method / Road Surface	RVS Length (km)	RVS Percentage (%)	CPX Length (km)	CPX Percentage (%)
Concrete	639.8	34.4	585.3	31.7
Dense Asphalt (SMA-S1)	466.9	25.1	477.3	25.8
Open-graded Asphalt (SMA-S3)	335.4	18.0	334.9	18.1
Others	418.8	22.5	449.9	24.4
Total	1860.9	100.0	1847.4	100.0

Acquisitions at transition joints or other highway discontinuities as well as during overtaking manoeuvres were discarded. The full set including auxiliary data was merged into $100\,\mathrm{m}$ sections, corrections were applied according to the appropriate standard:

- RVS: speed deviation, road temperature
- CPX: speed deviation, air temperature, tyre hardness, road surface, trailer

2.2 Pass-by Measurements

Due to past research projects regarding the acoustic performance of low-noise asphalts and grinding structures in concrete pavements these three types (i.e. porous asphalts, concrete & grinding) provide the main part of sites analyzed via the SPB-method, see table 3.

Table 3: Overview of the different road surfaces where stationary as well as trailer-based rolling noise measurements and were performed. Noted ages correspond to the moment of data acquisition of SPB-measurements .

Road Surface	Age (y)	Sites	Measurements 80 km/h	100 km/h
Concrete	0.9 – 30.4	9	9	8
Dense Asphalt (SMA-S1)	11.6 – 15.6	3	3	3
SMA-S2	8.6	1	1	1
Porous Asphalt (SMA-S3)	1.3 – 12.6	11	13	4
Grinding	0.04 – 2.8	6	10	9
Total	0.04-30.4	30	36	25

Acoustic data as well as the speed of a minimum of 120 cars and 80 heavy trucks, viz., each being a single pass-by event with a SPL rise/drop of 10 dB, was recorded. Additionally, controlled pass-bys (CPB) of an in-house vehicle equipped with a GPS sensor were likewise monitored and facilitated the speed measurement via radar. Within this range the overall L_{Aeq} and third-octave-band $L_{Aeq,i}$ of each vehicle were computed, subsequent linear models according to equations 1 and 2, respectively, allow the estimation of values corresponding to $80\,\mathrm{km/h}$.

$$L_{Aeq}(v) = a \cdot \log_{10}(v/v_0) + b \tag{1}$$

$$L_{Aeq,i}(v) = a_i \cdot \log_{10}(v/v_0) + b_i \tag{2}$$

$$\text{reference speed } v_0 = 50\,\mathrm{km/h}$$

2.3 Analysis Methods

In the following, Loess-regressions of overall SPL (for RVS∼CPX) and linear interpolations of overall and third-octave-band SPL (for RVS∼CPX and CPX∼SPB) are presented. Resulting cross correlations as well as PCA of each method allow investigations of possible frequency interrelations. The latter method further allows the analysis regarding possible dimension reductions and will be compared with a multivariate regression model. Finally it will be shown that LDA algorithms of CPX data facilitates the acoustic determination of the three most common road types.

3. TRAILER MEASUREMENT CORRELATIONS

Both SPLs (LMA≙RVS-levels, LCPX≙CPX-levels) are plotted pairwise for the complete data set (left) and filtered for the most prominent pavement types (right) in figure 3.

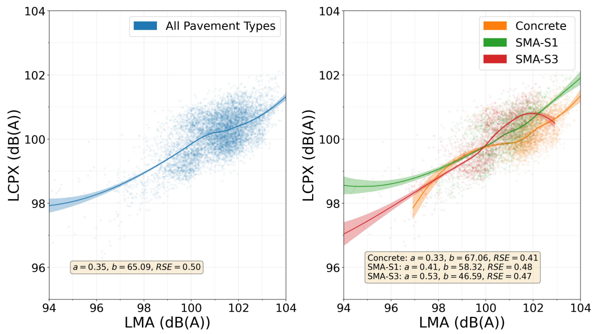

Figure 3: LCPX (CPX-measurement) and LMA (RVS-measurement) overall SPL correlations including data of all pavement types (left) and separated for concrete (orange), SMA-S1 (green) and SMA-S3 (red). Depicted Loess-regressions suggest non-linear relationships, however, given parameters from linear regressions show RSEs ≤ 0.5 dB.

Loess-regressions show non-linear relationships in the relevant level-regimes and produce only marginally decreasing residual standard errors (RSEs) when regarding concrete, SMA-S1 and SMA-S2 separately. This results in quite deviating coefficients of corresponding linear correlations according to equation 3.

$$\mathrm{LCPX} = a \cdot \mathrm{LMA} + b \tag{3}$$

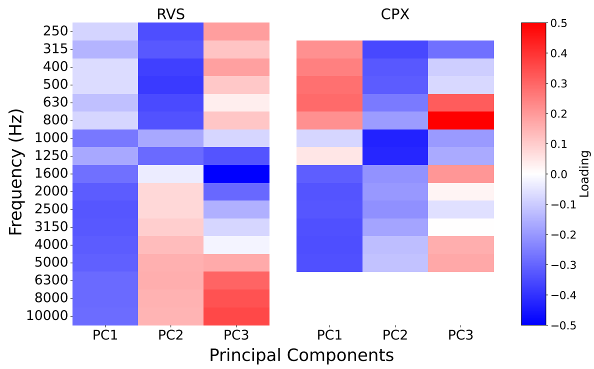

Figure 4: Principal Component Analysis of third-octave band SPLs of RVS (left) and CPX-measurements (right). The loading of each component is colour-coded.

Third-octave-band analyses via PCA is shown in figure 4. The RVS-method shows elevated loading vectors at PC1 and PC2 for higher and lower frequencies, respectively, while frequencies around 1000 Hz are less pronounced. Variances therefore show a heavy dependence on higher frequencies for RVS-levels, while the PCA of CPX-levels collapses to three regimes with limits at 1000 Hz and 1600 Hz. Linear cross correlations between both methods again depict low and high frequency regimes, see figure 5. Only direct interrelations are visible at 1000 Hz and 1250 Hz, respectively, but show relation to other third-octave bands. This is due to the distinct variation of shape and position of each method's maximum. Multiple reasons may be attributed to the above mentioned deviations:

- PIARC and SRTT tyre tread patterns differ from another considerably. Due to the former's smoothness (except for the four linear grooves) a reduced tangential vibration may be assumed [5]. This may consequently reduce noise emissions between 600 Hz and 3000 Hz.
- The deviating tread patterns may also have impact on the aerodynamic noise emission processes. Such processes, e.g. air pumping, also depend on wheel loads (RVS: 4000 N, CPX: 3200 N per tyre) and tyre pressures (RVS: 230 kPa, CPX: 200 kPa) [6].
- Regarding RVS-measurements, one of two microphones is positioned directly behind the tyre. Due to the Horn effect's angle and frequency dependent noise emission an elevated SPL between 1000 Hz and 1250 Hz can be expected. Additionally, only the rear microphone's level is considered in the overall RVS-SPL if the laterally positioned microphones level is lower. Energy-equivalent average values are computed otherwise.
- Both tracks of the inspected lane are recorded via the CPX-method. In contrast to the RVS-method local road conditions are therefore acoustically detected on both sides.
- Frequency dependent corrections with respect to the trailer geometry are applied to CPX-SPLs, however, no equivalent procedures are present in RVS 11.06.64.

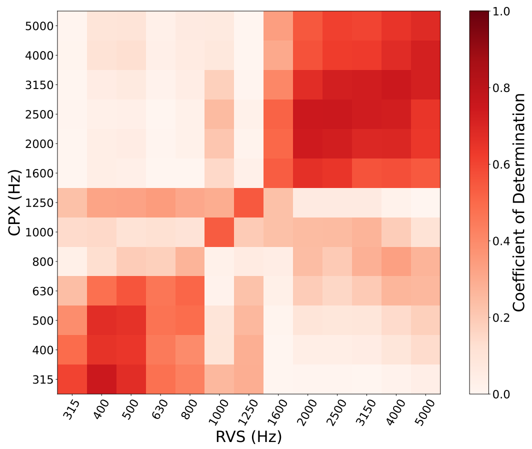

Figure 5: Color coded coefficient of determination for each linear correlation for each third-octave band of RVS- and CPX-measurements. Two distinct regimes are noticeable in the low and high frequency domain whereas only direct correlations for the center frequencies of 1000 Hz and 1250 Hz are given.

The colour-coded difference in days between both measurements exhibits an elevated gap of more than one year (depicted in yellow) for a minor fraction of the data set and were only measured at 80 km/h with the CPX-method. Novel Grinding pavement as well as aged asphalt and concrete sections result in a broad and uniformly packed dB-range. Nevertheless, the dataset of 30 is not exhaustive enough to provide correlations for specific pavement types. Reasonable coefficients of determination are obtained for passenger cars (cat1) and controlled pass-bys (CPB) while no significant correlation for heavy trucks (cat3) is given. Corresponding RSEs are listed in table 4.

Table 4: Residual standard errors from correlations of overall CPX-SPLs towards overall SPB-SPLs for passenger cars, trucks and controlled passbys.

	RSE (dB(A))	
Vehicle Type	80 km/h	100 km/h
passenger cars (cat1)	0.94	0.79
heavy trucks (cat3)	1.37	1.41
controlled pass-bys (CPB)	0.89	0.92

This can be attributed to the utilized SRTT-tyre whose tread pattern and acoustic emission corresponds to passenger vehicles. The slopes for all vehicles are higher for $80\,\mathrm{km/h}$ than for $100\,\mathrm{km/h}$. Differences of CPX-levels and SPB-levels thus heavily depend on the reference speed but also on pavement types, e.g. they have frequency dependent sound absorption properties, and has also been observed by Licitra et al. [7] and Sandberg et al. and [8]. Analogue analysis based on color-coded coefficients of determination resulting from separate third-octave band correlations has again been conducted for passenger cars and heavy trucks, see figure 6. The former shows two coarsely separable frequency domains with numerous significant interrelations below/above $1600\,\mathrm{Hz}$.

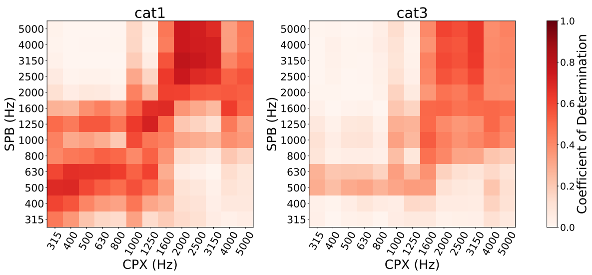

Figure 6: Color coded coefficient of determination for each linear correlation for each third-octave band of CPX- and SPB-measurements for passenger cars (cat1, left) and heavy trucks (cat3, right) at $80\,\mathrm{km/h}$. The loading of each component is colour-coded.

The latter clearly demonstrates the lack of application of the SRTT-tyre within the CPX-trailer regarding the typical rolling noise spectrum of heavy trucks for third-octave bands below $1600\,\mathrm{Hz}$. Figure 7 depicts the results of closer spectral analysis via PCA for both vehicle types, corresponding explained variances per principal component as well as spectral average values are shown in figure 8. PC1 for cat1 shows comparable loadings for cat1 and explains approx. 65% of variance. A substantially lower proportion of approx. 20% is explained via PC2, which further entails a distinction to three regimes for cars, dominated by high and low frequencies. Regarding heavy trucks PC1 already explains more than 80% of variance and loadings gradually increase with frequency. Reconsidering reasonable correlation coefficients between CPX- and SPB- measurements for both vehicle types in figure 6 multivariate regressions were conducted based on third-octave bands as well as the the first three CPX-PCs.

In order to gain insight into the performance of each model 30 varying permutations were computed for each speed and vehicle type, respectively, resulting in overall RSEs in table 5. Both regressions indeed provide reduced errors, however, since the number of considered third-octave bands is in the same size range as the analyzed datasets dimensions (see table 3) overfitting is not negligible.

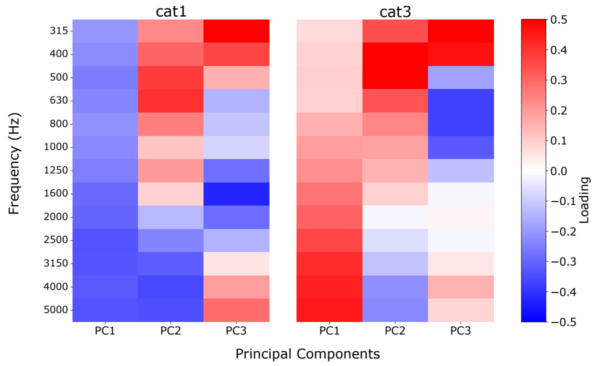

Figure 7: Principal component analysis for pass-bys of passenger cars (cat1, left) and heavy trucks (cat3, right). The loading of each component is colour-coded.

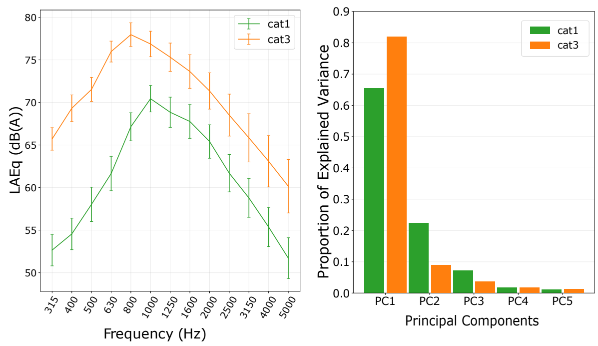

Figure 8: Frequency-dependent arithmetic means (left) and explained variance resulting from the PCA (right) for passenger cars (cat1, green) and heavy trucks (cat3, orange) at $80\,\mathrm{km/h}$. A peak shift from $800\,\mathrm{Hz}$ towards $1000\,\mathrm{Hz}$ between the two data sets and varying distributions result in elevated differences in the individual explained variances for each category.

Table 5: Average residual standard errors from 30 consecutive correlations of third-octave bands and PCA CPX-SPLs towards overall SPB-SPLs for passenger cars, trucks and controlled passbys.

Regression	Vehicle Type	RSE (dB(A))	
		$80\,\mathrm{km/h}$	$100\,\mathrm{km/h}$
Multivariate Regression	passenger cars (cat1)	0.64	0.40
	heavy trucks (cat3)	0.72	0.52
	controlled pass-bys (CPB)	0.68	0.44
PCA	passenger cars (cat1)	0.79	0.75
	heavy trucks (cat3)	1.14	1.25
	controlled pass-bys (CPB)	0.86	0.90

4. CONCLUSIONS

Two trailer-based tyre/road noise measurement techniques were performed along more than $1800\,\mathrm{km}$ within the Austrian highway network. Additional acoustic acquisition of single pass-bys of passenger cars and heavy trucks took place at 30 different measurement sites. Linear interpolation of overall SPLs resulted in RSEs$\leq 0.5\,\mathrm{dB}$ for RVS$\sim$CPX correlations. Analogue analysis resulted in speed dependencies for CPX$\sim$SPB correlation parameters. Significant relations are obtained for computations towards passenger car pass-bys, however, exhibited coefficients of determination are close to zero for heavy trucks. Similar regressions based on third-octave bands for both relations resulted in three distinct frequency regimes for RVS$\sim$CPX, two coarsely separable domains for CPX$\sim$SPB for passenger cars and some interrelations at higher frequencies for for heavy trucks.
PCAs of the trailer based methods further resulted in two coarse (RVS) and three clearly separable (CPX) ranges. Corresponding principal components for pass-bys of passenger cars and heavy trucks showed great dependency on frequencies starting at approx. $1600\,\mathrm{Hz}$. Closer analysis of CPX$\sim$SPB relations via multivariate regressions of third-octave bands as well as PC1-PC3 resulted in reduced RSEs for both speeds and all vehicle types, however, overfitting might have happened. To facilitate enhanced correlation qualities a more numerous dataset of SPB-measurements is inevitable. Furthermore, a new H1-tyre targeting the rolling noise of heavy trucks is of great need but currently unavailable.

5. ACKNOWLEDGEMENTS

Presented data was recorded within the research projects *INGGO* (funding: FFG - Austrian Research Promotion Agency, Mobility of the Future, MdZ - DACH 2016) *ADURA* (funding: FFG - Austrian Research Promotion Agency, Mobility of the Future, MdZ - DACH 2017) *ROSALIA* (funding: FFG - Austrian Research Promotion Agency, Mobility of the Future, MdZ - VIF 2019) The authors would like to thank the Autobahnen- und Schnellstraßen-Finanzierungs- Aktiengesellschaft (ASFiNAG), the Federal Ministry for Climate Action (BMK) as well as the Austrian Research Promotion Agency and the states for the support within the aforementioned projects.

6. REFERENCES

[1] Österreichische Forschungsgesellschaft Straße - Schiene - Verkehr (FSV): RVS 11.06.64: Berechnung von Schallemissionen und Lärmschutz, Wien, 1997

[2] International Organization for Standardization: ISO11819-2: Acoustics - Method for measuring the influence of road surfaces on traffic noise - Part 2: Close-proximity method, Geneva, 1997

[3] International Organization for Standardization: ISO11819-1: Acoustics - Measurement of the influence of road surfaces on traffic noise - Part 1: Statistical pass-by method, Geneva, 2017

[4] International Organization for Standardization: ISO11819-3: Acoustics - Method for measuring the influence of road surfaces on traffic noise - Part 3: Reference tyres, Geneva, 1997

[5] K. Larsson, S. Barrelet, W. Kropp Modelling of Tangential Contact Forces, Proc. of the 2nd Convention of the European Acoustics Association - Forum Acousticum, Techn Univ of Berlin, Berlin, Germany, 1999

[6] J. Eisenblaetter, S. J. Walsh, V. V. Krylov Air-related mechanisms of noise generation by solid rubber tyres with cavities, Applied Acoustics., 2010, **71**, 854-860

[7] G. Licitra, M. Cerchiai, L. Teti, and F. Bianco and M. Chetoni. Relationship between Pass By results, CPX ones and roadside long-term measures: some considerations, Internoise, Hamburg, 2016

[8] U. Sandberg, H. Kim. Evaluation of Noise Reduction of Korean Low-Noise Pavements – Part 2: Issues regarding the application of the CPX method, Internoise, Seoul, 2020